Global target analysis of picosecond chlorophyll fluorescence kinetics from pea chloroplasts

A new approach to the characterization of the primary processes in photosystem II α- and β-units

Theo A. Roelofs, Choon-Hwan Lee, and Alfred R. Holzwarth
Max-Planck-Institut für Strahlenchemie, Stiftstr. 34–36, D-4330 Mülheim a.d. Ruhr, Germany

ABSTRACT In this study, we have used the method of target analysis to analyze the ps fluorescence kinetics of pea chloroplasts with open (F_0) and closed (F_{max}) photosystem II (PS II) centers. Extending the exciton/radical pair equilibrium model (Schatz, G. H., H. Brock, and A. R. Holzwarth. 1988. *Biophys. J.* 54:397–405) to allow for PS II heterogeneity, we show that two types of PS II (labeled α and β) must be accounted for, each pool being characterized by its own set of molecular rate constants within the model. Simultaneous global target analysis of the data at F_0 and F_{max} results in a detailed description of the molecular kinetics and energetics of the primary processes in both types of PS II units. This characterization revealed that the PS IIα pool accounts for twice as many Chl molecules as PS IIβ, which suggests a PSIIα/PSIIβ reaction center stoichiometry of close to unity. By extrapolation it is shown that the primary charge separation in hypothetical "isolated" β reaction centers is slower than in isolated α reaction centers: in open centers by a factor of 4 ($1/k_1^{int}$ = 11 vs 2.9 ps), in closed centers by a factor of 2 ($1/k_1^{int}$ = 34 vs 19 ps). Despite this slower charge separation process in PS IIβ, the quantum efficiency of the charge separation process is hardly affected: a charge stabilization yield at F_0, (i.e., $P^+IQ_A^-$) of 86% (as compared to 90% in PS IIα). Reduction of Q_A (closing PS II) has distinctly different effects on the primary kinetics of PS IIβ, as compared to PS IIα. In PS IIα the charge separation rate drops by a factor of 6, whereas the charge recombination process is hardly affected. In PS IIβ the charge separation is slowed down by a factor of 3, whereas the charge recombination rate increases by a factor of 5. In terms of changes in standard free energy, the reduction to Q_A^- lifts the free energy of the radical pair P^+I^-, relative to the excited state $(Chl_n/P)^*$, by 47 meV in PS IIα and by 67 meV in PS IIβ. The concomitant increase in fluorescence quantum yield is the same for both types of PS II. These results show that PS IIα and PS IIβ exhibit a different molecular functioning with respect to the primary processes, which might have its origin in a different molecular structure of the reaction centers and/or a different local environment of these centers. Location in different parts of the thylakoid membrane might be involved. We also applied different error analysis procedures to determine the error ranges of the values found for the molecular rate constants. It is shown that the commonly used standard error has very little meaning, as it assumes independence of the fit parameters. Instead, an exhaustive search procedure, accounting for all possible correlations between the fit parameters, gives a more realistic view on the accuracy of the fit parameters.

INTRODUCTION

In the energy conversion process of higher plant photosynthesis light energy captured by photosystem II (PS II) ultimately leads to the electron transfer from water to plastoquinone. Chlorophyll (Chl) antenna pigments harvest light and transfer the excitation energy to the reaction center complex, the site of primary photochemistry in PS II. In the reaction center, a special Chl dimer, P, gets excited and is subsequently photo-oxidized by transferring an electron to a pheophytin molecule, I, within ~3 ps (1–3). A further charge stabilization step, electron transfer from I^- to the primary plastoquinone Q_A, leads to the charge separated state $P^+IQ_A^-$, within several hundreds of picoseconds (4–6). From Q_A^- the electron is transferred to a secondary plastoquinone Q_B. The oxidized donor P^+ is re-reduced by a tyrosine residue, called Z, (7, 8), which ultimately receives an electron from the water splitting complex. If the electron acceptor Q_A is already reduced, the corresponding charge stabilization step cannot take place and the fate of the radical pair P^+I^- is to recombine, yielding either the excited state of the donor, P^*, or the triplet state of the donor (if spin dephasing processes occur during the lifetime of the radical pair, [9]), or the ground state. For reviews on the electron transfer processes in PS II see (10, 11).

Address correspondence to Dr. Holzwarth.
Dr. Roelofs' present address is Laboratory of Chemical Biodynamics, Lawrence Berkeley Laboratory, University of California at Berkeley, Berkeley, California 94720.
Dr. Lee's present address is Department of Molecular Biology, Pusan National University, Pusan, 609-735, Korea.

Modeling the primary processes in PS II

The kinetics of the primary photophysics and photochemistry of PS II has been studied by various time-resolved

methods, such as absorption, fluorescence and photovoltage techniques. Based on these experimental results, several kinetic models have been proposed to describe the excited state dynamics in PS II. These models can be classified into two main categories, when the key features of these models are considered. The first category of diffusion-limited kinetic models has the bipartite model as central element. The bipartite model (12) describes the energy transfer from the antenna to the reaction center as a reversible process, whereas the charge separation is considered to be irreversible and is described by one rate constant which is supposed to be much faster than those for the energy transfer steps. This model predicts biexponential fluorescence decay kinetics for the excited states in the antenna. The bipartite model has been extended to account explicitly for a heterogeneous antenna system (tripartite model, [13]) or for a heterogeneous pool of PS II systems (heterogeneous bipartite model, [13, 14]). The group of Butler and co-workers, who proposed these models and fitted them to stationary and time resolved fluorescence data, concluded that from the three variants the heterogeneous bipartite model is most appropriate for chloroplasts (14).

A basically different model for the excited state dynamics in PS II, called the exciton/radical pair equilibrium model, has been presented by Holzwarth and co-workers (1, 15). In Fig. 1 this model is shown in a comprehensive form. It describes a trap-limited exciton decay ($k_t, k_{-t} \gg k_1$) and an equilibrium between P^* and P^+/I^- (k_1 and k_{-1}). In open centers (Q_A oxidized) k_2 describes the sum of the charge stabilization process (electron transfer from I^- to Q_A) on the one hand, and recombination of the (singlet) radical pair P^+I^- back to the ground state and triplet radical pair formation, on the other hand. As fluorescence spectroscopy only monitors the excited state $(Chl_n/P)^*$, these processes can not be distinguished from each other: k_2 describes the sum of these three processes. In closed centers (Q_A^-) the rate constant k'_2 is used, which solely describes the processes of radical pair recombination back to the ground state and the spin dephasing processes leading to the triplet radical pair state. The model predicts biexponential fluorescence decay kinetics for the equilibrated $(Chl_n/P)^*$ state (Fig. 1 *B*). The reversible energy partition between excited state and radical pair, first suggested in (10, 15), is experimentally supported by the correspondence of one of the fluorescence lifetime components to the lifetime of the radical pair P^+I^-, as revealed by picosecond absorption (5) and picosecond photovoltage (16, 17) measurements.

The two main kinetic models for PS II, the bipartite model and the exciton/radical pair equilibrium model, both formally predict biexponential fluorescence kinetics. However, the physical interpretation of the rate constants is basically different.

The excited state dynamics in PS II has recently been reviewed (18) and it has been shown that the fluores-

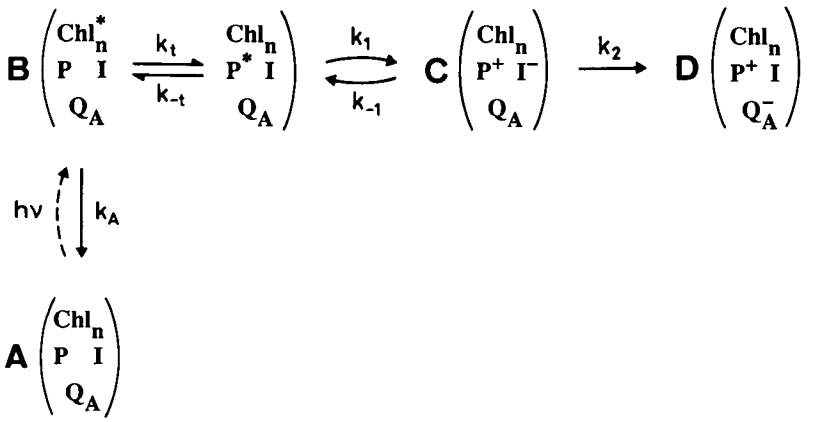

FIGURE 1 Exciton/radical pair equilibrium model for the primary processes in PS II, as presented previously (1). The model is in principle characterized by four rate constants: k_1 is the apparent rate constant for the primary charge separation; k_{-1} describes the radical pair (P^+I^-) recombination back to the excited state of the donor P^*; k_2 (at F_0) is the overall rate constant for the charge stabilization from I^- to Q_A on one hand, and the recombination of the singlet radical pair back to the ground state and triplet radical pair formation on the other hand. At F_{max}, k'_2 solely describes the recombination of the radical pair back to the ground state and spin dephasing processes leading to the triplet radical pair state. k_A describes the overall (i.e., radiative and radiationless) decay of excited states in the Chl antenna complex. Furthermore, k_t and k_{-t} describe forward and backward energy transfer from the Chl antenna to the primary donor P in the reaction center. It is assumed that $k_t, k_{-t} \gg k_1$ (i.e., trap-limited exciton decay; see text), so that we can use the generalized excited state $(Chl_n/P)^*$, state *B*. Allowing for heterogeneity of PS II is done by considering two independent exciton/radical pair equilibrium model systems.

cence kinetics found in several laboratories agree quite well with each other, whereas the interpretations of these kinetics are substantially different. It was discussed there extensively, why we think that the exciton/radical pair equilibrium model is the most appropriate description at present (see [18] and references there in). In this report, we only want to mention some additional lines of evidence supporting this model. The first one has been shown by McCauley et al. (19) who reported ultrafast blue-shifted fluorescence in pea chloroplasts. They found that upon excitation at 692 nm (i.e., red shifted relative to the PS II emission maximum around 682 nm), the complete emission spectrum and decay kinetics are recovered (as compared to excitation at 630 nm) within ~15 ps. This directly shows that the equilibration of the excited states in the antenna of PS II takes place on a time scale (tens of ps) much faster than the primary photochemistry. A similar exciton equilibration lifetime component has also been found in green algae (Bittersmann and Holzwarth, in press). Another line of evidence was revealed by time-resolved photovoltage experiments. Leibl et al. (17) concluded from extensive analyses of picosecond photovoltage and fluorescence data, in terms of reversible and irreversible reaction schemes for charge separation in PS II, that only the reversible scheme can account for all the data available. These results further favor the exciton/radical pair equilibrium model over the (heterogeneous) bipartite model.

Picosecond fluorescence kinetics of thylakoids

Fluorescence decay kinetics of chloroplasts both at F_0 and F_{max}, published by several research groups during the last decade, have mostly been analyzed as a sum of three (sometimes four) exponential lifetime components (see 18, 20, 21 for reviews). The fastest component (~100 ps at F_0 and F_{max}) was thought to result mainly or exclusively from PS I. The two other components (~0.3 ns and 0.60 ns at F_0, 1.0 ns and 2.5 ns at F_{max}) were attributed to (two different types of) PS II. More recently, global lifetime analyses of fluorescence decays of green algae with a highly improved signal-to-noise ratio revealed that under conditions of F_{max} three components originating from PS II could be resolved (22). Lifetimes of 0.38 ns, 1.3 ns and 2.1 ns have been attributed to PS II (besides a 0.10 ns component attributed to PS I). For the situation at F_0, it has also been suggested that more than two lifetime components originate from PS II. By comparing the decay-associated spectrum (DAS) of the ~0.10 ns component under conditions of F_0 with that at F_{max}, McCauley et al. (23) concluded that this component actually is a composite of PS I and PS II contributions, as already had been suggested by others (14, 24).

Modeling the primary processes in thylakoids

The presence of a third PS II fluorescence lifetime component, both at F_0 and at F_{max}, forces us to reevaluate the interpretation of the fluorescence kinetics of intact thylakoid membranes from higher plants and green algae. In this study we extend the exciton/radical pair equilibrium model, to account for a heterogeneity of PS II. Each pool of PS II is described by its own set of rate constants, or equivalent, by its own biexponential decay kinetics. An alternative extension of the exciton/radical pair equilibrium model could be the introduction of a relaxed radical pair state, formed out of the primary radical pair, by a (reversible) relaxation process. Such a model predicts triexponential fluorescence decay kinetics. However, in a previous study on whole cells of green algae (22) we already demonstrated that this model does not apply to intact PS II and therefore it will not be considered here any further.

The heterogeneous exciton/radical pair equilibrium model used here predicts four PS II fluorescence lifetime components, both at F_0 and F_{max}. Additionally, a PS I component and an exciton equilibration component (vide supra) can be expected. This means that (at least) six fluorescence lifetime components are expected, both at F_0 and F_{max}. However, fitting fluorescence decays as a sum of exponentials is limited in the number of components that can be resolved, because of its intrinsically ill-posed problem. Therefore, a more powerful data analysis method had to be used to extract more information from the experimental data. We apply here the concept of global target analysis (25, 26). The essence of target analysis is that explicit kinetic models are tested for compatibility with the experimental data. The set of rate constants describing the kinetic model is directly fitted to the data. This results in more constraints to the fit, as compared to fitting with a sum of uncorrelated exponentials (25, 26). To account for those fluorescence processes occurring in thylakoids, which are not explicitly described by the model (vide supra) extra exponential components are added to the kinetics of the model.

Our working hypothesis and notation used throughout this paper assumes that the two PS II pools used in the heterogeneous exciton/radical pair equilibrium model correspond to PS IIα and PS IIβ (27). The concept of the α/β-heterogeneity of PS II is based on the kinetic analysis of the fluorescence induction signals in the presence of DCMU (28). We should like to stress the point, that the kinetic analysis performed here is in fact independent of this hypothesis.

MATERIALS AND METHODS

Samples

Chloroplasts were isolated according to Glick et al. (29) from the leaves of 12–14 day-old pea plants. For fluorescence decay measurements, the chloroplasts were diluted in buffer (0.4 M sucrose, 10 mM NaCl, 5 mM $MgCl_2$ and 25 mM Tricine, pH 7.8) to a final concentration of 10 μg Chl/ml. The sample (1 L) was thermostated at 4°C, kept in the dark and pumped through a flow cuvette (cross-section 1.5 × 1.5 mm) with a flow speed of ~300 ml/min. The F_0-state was maintained by dark adaptation and a sufficiently low excitation intensity; F_{max} was reached by addition of 1 mM hydroxylamine, 1 μM gramicidin and 20 μM DCMU, in combination with actinic illumination by moderate intensity of white light just before entering the flow cuvette. Aliquots were taken from the sample at the beginning and the end of each measurement and the fluorescence induction signals (in the presence of DCMU) were recorded, to check for sample damaging and/or aging during data collection (typically 75 min.). No effect of aging or damaging was found.

Fluorescence decays

Fluorescence decay kinetics were measured with the single photon timing technique, using the set up described previously (30). The sample was excited at 630 nm by laser pulses with a full width at half maximum (FWHM) ≤15 ps, at a repetition rate of 800 kHz. The fluorescence was selected by a double monochromator (spectral bandwidth 4 nm FWHM) and detected by a R-955 photomultiplier (Hamamatsu, Iwata-gun, Japan). This yielded a system response function of ~190 ps FWHM. The resolution of the time-to-amplitude converter was 10 ps/channel. After appropriate deconvolution of the decay curves with the system response function, a time resolution of ~20 ps could be achieved. Decays were recorded between 680 and 730 nm, with 65,000 counts in the peak channel at F_{max}, and 45,000–65,000 counts in the peak channel at F_0.

Data analysis

The fluorescence decay data were analyzed by two different procedures: global lifetime analysis and global target analysis. The data were fitted over a window of 10 ns and 6 ns for F_{max} and F_0 conditions, respectively. In the global lifetime analysis procedure (described in detail previously [30]) the fluorescence decays were fitted with a sum of exponentials, assuming that over a certain spectral range the excited state relaxation kinetics of a chromophore are constant: $F(t, \lambda_{em}) = \Sigma_{i=1}^{n} A_i(\lambda_{em}) \cdot \exp(-t/\tau_i)$. This allows the combined analysis of fluorescence decays detected at different wavelengths λ_{em}. The spectral constraint improves the resolution of the kinetics originating from spectrally different (groups of) chromophores. In this study it should allow particularly for a better resolution of the PS I kinetics and the exciton equilibration component, because their emission maxima are red-shifted as compared to the PS II spectrum (19, 30, 31). The fit quality was assessed by reduced χ^2-values, weighted residual plots and the corresponding autocorrelation functions. The results were presented as decay-associated spectra (DAS), i.e., as plots of the amplitudes A_i for the lifetime component τ_i versus the emission wavelength λ_{em}.

In the global target analysis procedure a (heterogeneous) excited state/radical pair equilibrium model (Fig. 1) was fitted to the decay curves. As the model assumes trap-limited exciton decay, the rate constants k_t and k_{-t} are not taken into account explicitly. Instead, an additional exponential component was allowed for, to describe the process of exciton equilibration within the generalized $(Chl_n/P)^*$ state (vide supra). The set of coupled differential equations has been solved analytically (1). To arrive at a unique solution one of the four rate constants has to be fixed (see 22 for a detailed discussion). In this study we fixed the rate constant k_A to a value of 0.3 ns^{-1}, which corresponds to a fluorescence lifetime of the (hypothetical) isolated Chl protein antenna complex of 3.3 ns (which is compatible with experimental data available on LHCP II [32, 33]). We used this value both for F_0 and F_{max}, because this rate constant is thought to remain unchanged upon reduction of Q_A. At F_0-conditions the results were only weakly depending on the value assumed for k_A, whereas at F_{max} this dependence is quite pronounced (1, 22). However, in combination with the kinetic model applied in this study, an upper limit for k_A of 0.5 ns^{-1} was found. Higher values for k_A led to negative values for one or more of the other rate constants, which is physically meaningless. Much lower values for k_A would be incompatible with the lifetime data of isolated Chl antenna complexes (vide supra).

Each of the two PS II pools is characterized by its own set of rate constants (k_A, k_1, k_{-1}, and k_2 or k_2') and by an amplitude factor which is proportional to the number of Chls connected to each pool. To account for the fluorescence decay components not incorporated into the model (i.e., PS I and exciton equilibration) exponential components (lifetime τ_i and preexponential factor A_i) were added to the kinetics of the model. In analogy to the global lifetime analysis, it was assumed that decays detected at different wavelengths can be described by the same set of kinetic parameters. Furthermore we constrained the amplitude of the lifetime component for PS I to be positive over the whole spectrum.

All the kinetic parameters, as well as the amplitude factors for the different PS II pools and the preexponential factors of the additional lifetime components were fitted directly to the experimental decay curves by a nonlinear Levenberg-Marquardt algorithm (34) (ZXSSQ routine from the IMSL Fortran Library), which minimizes the sum of the squared weighted residuals over all data points. The fit quality was evaluated by its reduced χ^2-values and plots of the weighted residuals and their autocorrelation functions. The results are presented as values for the rate constants k_i, the amplitude factors for the two pools of PS II, DAS of the corresponding lifetime components and DAS of the additional lifetime components.

Error analysis

The error ranges found for the optimal set of fit parameters depend strongly on the error analysis procedure performed (26, 35). We applied here two kinds of error analysis: a so-called unidimensional search procedure and an exhaustive search procedure (26). In the former procedure, no correlation between the fit parameters was accounted for, whereas in the latter, all possible (first and higher order) correlations were considered. In a unidimensional search the recovered fit parameters were altered along each independent parameter axis, until the new reduced χ^2-value was significantly worse than χ^2_{min}, the value corresponding to the optimal solution. The recovered error ranges could be asymmetric, in contrast to the commonly used ± standard error, which is calculated from the curvature matrix at χ^2_{min}. In the unidimensional search procedure the curvature of the χ^2-surface in the vicinity of its minimum was explored explicitly.

In the exhaustive search procedure the rate constant k_i was changed (increased or decreased) from its optimal value by a certain fraction. Subsequently, a new minimization of χ^2 was performed in which k_i is fixed, whereas all other fit parameters were allowed to relax, in order to find a new minimum on the reduced χ^2-surface. The rate constant k_i was thus increased/decreased stepwise until the new minimal value for the reduced χ^2 was significantly worse than χ^2_{min}. This procedure mapped the complete χ^2-surface around χ^2_{min}. It provided error ranges for each rate constant, at a given statistical accuracy. These error ranges could be asymmetric. It has to be stressed here that only in the

(ideal) case of complete absence of any correlation between the fit parameters, both search procedures would recover the same error ranges. Otherwise, the exhaustive search will result in much larger error ranges, or in other words, the unidimensional search will underestimate the error ranges to an extent that depends on the existing correlations between the fit parameters.

As to the question of the significance of a decrease in fit quality, it has been shown that the ratio of two reduced χ^2-values is distributed according to an *F*-distribution (36). For the given number of degrees of freedom (i.e., number of data points minus number of free-running fit parameters) and a preset confidence level (of 67% in our case, roughly corresponding to one standard deviation), we calculated the *F*-factor by which χ^2_{min} was allowed to increase, before this increase had to be considered as significant. Vice versa, for a given χ^2-value ($> \chi^2_{min}$) we could calculate the confidence level with which we could qualify this value to be significantly worse than χ^2_{min}. We used the routines FDF and FIN (IMSL Fortran Library) to generate *F*-distributions.

RESULTS AND DISCUSSION

Global lifetime analysis

For fitting the fluorescence kinetics (eight decays detected at eight different wavelengths) from pea chloroplasts with open PS II reaction centers (F_0) by global lifetime analysis, five lifetime components were needed. The global reduced χ^2-value for this fit is 1.03. The weighted residuals plots and corresponding autocorrelation functions are shown in Fig. 2, which demonstrates the good quality of the fit. The corresponding DAS are shown in Fig. 3 (upper part). The fastest component, τ = 20 ps has a dominant amplitude between 690 and 730 nm. We attribute this component to the exciton equilibration process within the Chl antenna complexes from PS I and PS II, as discussed previously (19, 23). The time resolution in the present experiment ($\sim$20 ps) does not allow for a very accurate resolution of this component. However, in the light of previous work in our laboratory, carried out with higher time resolution, this assignment appears to be justified. The second lifetime component, τ = 104 ps, shows a DAS that peaks at $\sim$690 and 730 nm, and is therefore attributed mainly (vide infra) to PS I emission. The third and fourth lifetime components, τ = 0.29 ns and τ = 0.63 ns, have similar DAS that peak around 685 nm and are therefore attributed to PS II.

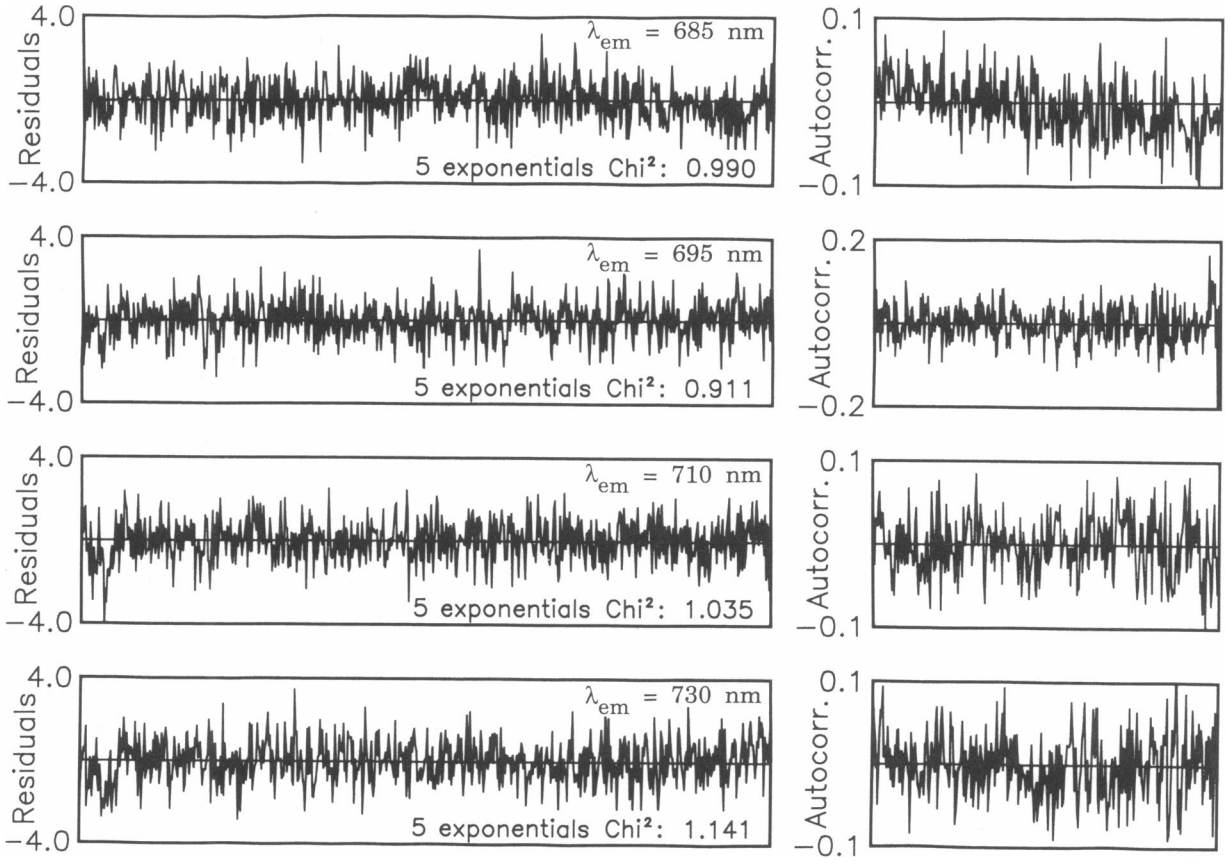

FIGURE 2 Weighted residuals plots and corresponding autocorrelation functions from the five component global lifetime analysis of the fluorescence kinetics of pea chloroplasts at F_0. The decays were fitted over a time window of 6 ns.

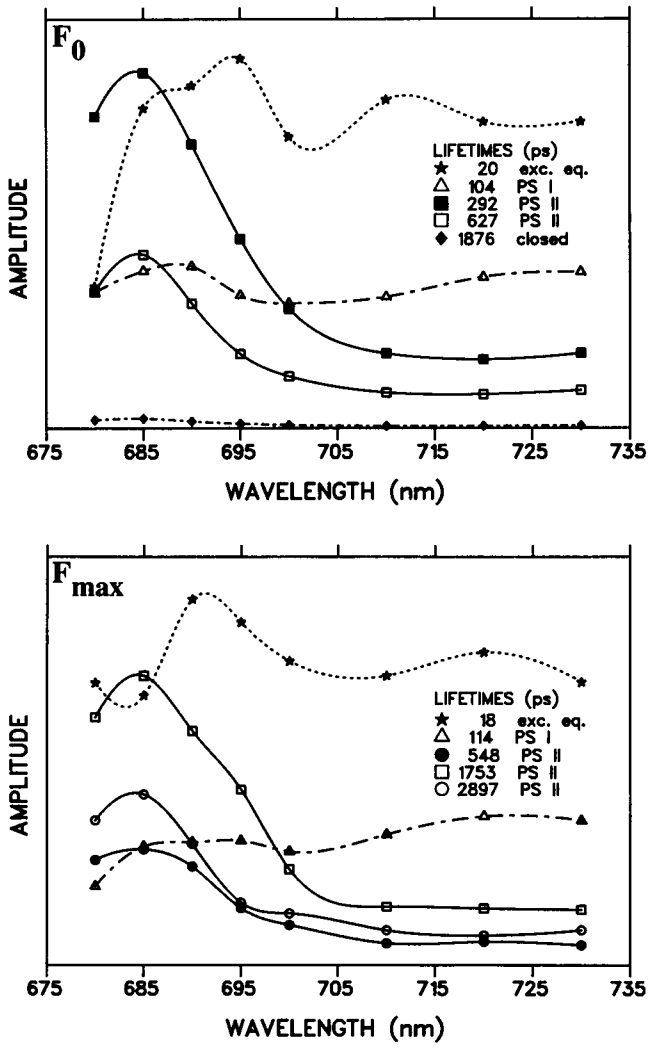

FIGURE 3 DAS of pea chloroplasts at F_0 and F_{max}, as calculated from the corrected amplitudes of the lifetime components in the global lifetime analyses. The curves between the data points are interpolated with third-order polynomials.

The fifth lifetime component, τ = 1.88 ns has a very small relative amplitude ($\leq 1\%$) and its DAS has the maximum also around 685 nm. The relative amplitude of this component could be further decreased by decreasing the effective excitation light intensity (i.e., either by attenuation of the laser pulses or by increasing the flow speed of the sample through the measuring cuvette). Therefore, we attribute this lifetime component to a small fraction of closed PS II. These lifetimes are in accordance with and the assignment of the individual components is based on previous work both by us and other laboratories (18).

For fitting the fluorescence kinetics at F_{max} also five exponential components are needed. The global reduced χ^2-value for this fit was 1.05 and the weighted residuals plots were free of any significant deviations from a random distribution (not shown). The DAS corresponding to this fit are shown in Fig. 3 (*lower part*). The fastest lifetime component, τ = 18 ps has a dominant amplitude over the whole spectrum, with maxima at ~690 and 720 nm and is again attributed to the exciton equilibration process in the PS I and PS II Chl antenna complexes (vide supra). The DAS of the second component, with a lifetime of 114 ps, shows two bands around 690 nm and 730 nm. This component is therefore again attributed to PS I emission. Comparing this DAS with that of the corresponding lifetime component at F_0 (τ = 104 ps), one notices that on going from F_0 to F_{max} the amplitude around 685–690 nm is decreased, relative to the band at 730 nm. This indicates that this component at F_0 probably is a composite of PS I and PS II emission, as has already been suggested previously (14, 23, 24). Closing the PS II centers increases the PS II lifetime and thus results in a better resolution of the pure PS I emission component. The three other lifetime components at F_{max}, τ = 0.55 ns, 1.75 ns and 2.90 ns, all have similar DAS with their maxima around 685 nm. These three components are therefore attributed to PS II. Compared to our previous results on pea chloroplasts at F_{max} (23, 37), we have resolved a third PS II emission component. This has been enabled by the drastically improved signal/noise ratio of the data collected in this study (65,000 counts in the peak channel for all decays, as compared to typically ~20,000 counts in previous work). To check whether the two PS II lifetime components reported in previous studies can indeed be considered to be a mixture of the three PS II lifetime components resolved here, we performed a global lifetime fit to the new data, allowing for only two PS II components. This yielded two PS II components with lifetimes of 1.11 and 2.51 ns, with the shorter one having about half the amplitude of the longer one. Both lifetimes, as well as their amplitude ratio, are in good agreement with the former results (23, 37). However, in our case this four component fit gave a drastically increased value for the reduced χ^2 (1.58 as compared to 1.05) and led to significant deviations in the weighted residuals plots (not shown). We note here that for green algae at F_{max} also three PS II lifetime components have recently been resolved, with lifetimes of 0.38 ns, 1.34 ns and 2.08 ns (22).

Global target analysis

As discussed above, we fitted a heterogeneous exciton/radical pair equilibrium model (Fig. 1) to the data. Unfortunately, we found more than one minimum for the separate global target analysis of F_0 and F_{max} data.

Depending on the starting values used for the different fit parameters, two solutions of comparable quality were found for open PS II centers, whereas for closed PS II centers even three qualitatively similar minima were found. These five different solutions for F_0 and F_{max} are collected in Table 1. For the assignment of α and β to the two different pools of PS II assumed in this target analysis, we postulate that the majority of the PS II Chls are connected to PS IIα. The two solutions for the F_0-case mainly differ in the value for k_{-1} of the α-centers and k_2 of the β-centers. In the lifetime domain, this reflects an interchange of identity for two of the lifetime components. This interchange is accompanied by a drastic change in A_α/A_β-amplitude ratio: 4.1 as compared to 1.0. In case $F_0(1)$, only 20% of the emitting Chls are coupled to PS IIβ, whereas in case $F_0(2)$, this fraction is 50%. The reduced χ^2-values differ by only a factor of 1.0025 (corresponding to a confidence level of 54%). In Fig. 4 (*upper left*), we show the weighted residuals plots and corresponding autocorrelation functions for the $F_0(1)$-case, which indicate that this fit is satisfactory. The corresponding plots for the $F_0(2)$-case are very similar (not shown). For the situation at F_{max}, three minima were found. These three solutions differ in the value for k_{-1} of α-centers and in all the three rate constants for β-centers. The case $F_{max}(2)$ seems to be the odd one out, as in this case k_{-1} for PS IIβ is extremely large, as compared to k_1, which is reflected in an almost mono-exponential fluorescence decay (the fastest lifetime component for PS IIβ has a relative amplitude of only 0.2%). The reduced χ^2-value of this case is higher than that of $F_{max}(1)$ by a factor of 1.0069 (corresponding to a confidence level of 62%). The fit qualitites for $F_{max}(1)$ and $F_{max}(3)$ are almost identical. In Fig. 4 (*lower left*), the weighted residuals plots and corresponding autocorrelation functions for the $F_{max}(1)$-case are shown, which demonstrate the satisfactory quality of this fit. The corresponding plots for the cases $F_{max}(2)$ and $F_{max}(3)$ are again very similar (not shown).

At this point, it seems appropriate to refer to our preliminary report on the separate global target analysis of the fluorescence kinetics from green algae at F_0 and F_{max} (38). It is known by now, that also in the separate analysis of these data, more than one solution is found to exist. The solutions presented in our previous report (38), were obtained by separate global target analyses of data at F_0 and F_{max} and could be compared with some of the cases presented in Table 1 (cf cases $F_0(1)$ and $F_{max}(2)$ in Table 1). An analogously detailed analysis of the kinetic data from green algae will be topic of a later manuscript.

Is PS II indeed heterogeneous?

To demonstrate that indeed (at least) two pools of PS II were needed to describe the fluorescence kinetics at F_0 and F_{max}, in terms of the exciton/radical pair equilibrium model, we also performed separate target analyses allowing only for a single homogeneous pool of PS II. When the decay kinetics in F_0 were fitted with a

TABLE 1 Results from the separate target analyses of the fluorescence kinetics of pea chloroplasts at F_0 and F_{max}

Case	Lifetimes PS IIα	PS IIβ	PS I	eq.[1]	closed[2]	Rate constants PS IIα k_1	k_{-1}	k_2, k'_2	PS IIβ k_1	k_{-1}	k_2, k'_2	A_α/A_β	χ^2
	(ns)						(ns^{-1})						
F_0													
$F_0(1)$	0.24, 0.45 (26%, 19%)	0.064, 0.78 (5%, 7%)	0.098 (7%)	0.016 (35%)	2.09 (0.6%)	3.0	0.29	2.8	7.1	7.2	2.5	4.1 ± 0.4	1.0222
$F_0(2)$	0.22, 0.64 (17%, 14%)	0.061, 0.33 (5%, 22%)	0.098 (6%)	0.016 (35%)	1.90 (0.8%)	2.9	0.80	2.2	5.2	5.2	8.6	1.0 ± 0.1	1.0248
F_{max}													
F_{max}	0.65, 1.79 (7%, 27%)	0.38, 2.92 (5%, 15%)	0.11 (9%)	0.013 (37%)		0.47	0.34	0.99	0.62	1.6	0.46	1.9 ± 0.4	1.0747
$F_{max}(2)$	0.56, 1.84 (11%, 31%)	0.097, 3.05 (0.2%, 13%)	0.11 (12%)	0.013 (34%)		0.58	0.52	0.92	0.20	8.5	1.7	3.7 ± 0.7	1.0821
$F_{max}(3)$	0.45, 1.71 (6%, 25%)	0.62, 2.84 (5%, 17%)	0.11 (10%)	0.013 (36%)		0.61	0.70	1.2	0.34	0.82	0.52	1.6 ± 0.3	1.0750

The relative amplitudes at 685 nm for the lifetime components are given in parentheses. The values given for the amplitude ratios A_α/A_β are the average ± standard deviation over the whole emission spectrum, as no significant correlation was found between the emission wavelength and A_α/A_β (Note that in the fit procedure itself, these parameters were allowed to vary over the spectrum). [1]Lifetime component reflecting the exciton equilibration process. [2]Lifetime component reflecting a small fraction of closed PS II centers.

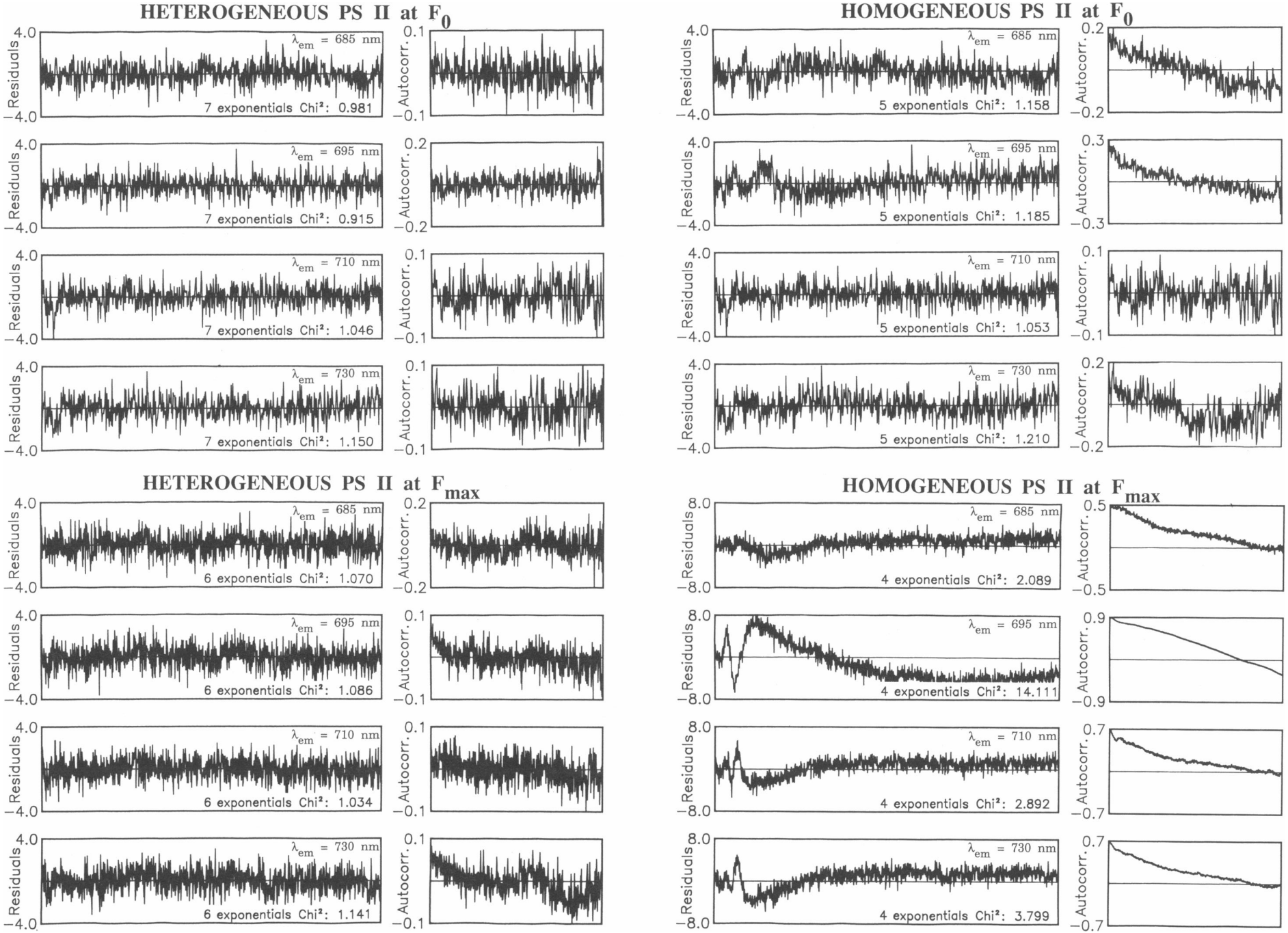
HETEROGENEOUS PS II at F_0
HOMOGENEOUS PS II at F_0
HETEROGENEOUS PS II at F_{max}
HOMOGENEOUS PS II at F_{max}
Residuals
Autocorr.
λ_{em} = 685 nm
λ_{em} = 695 nm
λ_{em} = 710 nm
λ_{em} = 730 nm
7 exponentials Chi²: 0.981
7 exponentials Chi²: 0.915
7 exponentials Chi²: 1.046
7 exponentials Chi²: 1.150
5 exponentials Chi²: 1.158
5 exponentials Chi²: 1.185
5 exponentials Chi²: 1.053
5 exponentials Chi²: 1.210
6 exponentials Chi²: 1.070
6 exponentials Chi²: 1.086
6 exponentials Chi²: 1.034
6 exponentials Chi²: 1.141
4 exponentials Chi²: 2.089
4 exponentials Chi²: 14.111
4 exponentials Chi²: 2.892
4 exponentials Chi²: 3.799

homogeneous PS II pool, the values found for the rate constants were $k_1 = 2.7\ ns^{-1}$, $k_{-1} = 0.34\ ns^{-1}$ and $k_2 = 2.1\ ns^{-1}$. This is equivalent to lifetimes of 0.27 ns (32%) and 0.59 ns (18%) (relative amplitudes at 685 nm given in parentheses). Additionally, three components with lifetimes of 0.018 ns (41%), 0.097 ns (8%) and 1.74 ns (1%) were resolved. The reduced χ^2-value for this fit is 1.0979 and the weighted residuals plots and corresponding autocorrelation functions are shown in Fig. 4 (*upper right*). As compared to the plots allowing for two different PS II pools (Fig. 4, *upper left*), the improvement of the fit quality is evident. In the homogeneous fit, the weighted residuals plots and more pronounced, the autocorrelation functions show significant deviations from random distribution, especially in the PS II emission spectral region (680–695 nm), which disappear when allowing for two pools of PS II. Fitting the F_{max} data with a homogeneous PS II pool resulted in PS II rate constants of $k_1 = 0.28\ ns^{-1}$, $k_{-1} = 1.9\ ns^{-1}$ and $k'_2 = 0.50\ ns^{-1}$, which is equivalent to lifetimes of 1.15 ns (24%) and 2.51 ns (37%). In addition, components with lifetimes of 0.042 ns (28%) and 0.20 ns (11%) are found. The reduced χ^2 for this fit was 3.60 and the weighted residuals and autocorrelation functions are plotted in Fig. 4 (*lower right*). Comparing the quality of the fit with a homogeneous PS II pool (Fig. 4, *lower right*) with that of a heterogeneous pool (Fig. 4, *lower left*), the necessity for taking into account at least two different PS II pools becomes even more evident. Of course, we can not exclude more than two different pools of PS II, but the present data do not give any indications for that.

Comparison between global target analysis and global lifetime analysis

It is interesting to compare the quality of a global target fit, using the exciton/radical pair model for a homogeneous PS II pool, with that of a global lifetime fit, using a sum of uncorrelated exponentials. For open PS II centers, both procedures describe the fluorescence decay kinetics of chloroplasts as a sum of five exponential components. Comparing the corresponding weighted residual plots and reduced χ^2-values, Fig. 4, (*upper right*) and Fig. 2, respectively, it becomes clear that these five exponential components are sufficient to get a good fit only if these components are completely unconstrained (Fig. 2). However, by the global target analysis procedure, constraints are put on the individual components by the explicit kinetic model, which correlates the individual exponential components with each other, and thus limits the multidimensional solution space. These additional constraints enable to extract more information from the decay curves (in this case a PS II heterogeneity), which demonstrates one of the main merits of target analysis.

FIGURE 4 Weighted residuals plots and corresponding autocorrelation functions from the separate global target analysis of the fluorescence kinetics of chloroplasts at F_0 and at F_{max} analyzed as a heterogeneous or a homogeneous PS II pool. The decays in F_0 were fitted over a time window of 6 ns, the F_{max} decays over a time window of 10 ns.

Combined global target analysis of the kinetics at F_0 and F_{max}

Before we can characterize the two types of PS II, we have to come to a unique solution for the fit parameters. The procedure used above provided two solutions at F_0 and three at F_{max} (see Table 1), which in principle allows for composing six combinations of F_0 and F_{max} kinetics. By applying two additional, physically and physiologically reasonable constraints, we tried to arrive at a unique solution. The first of these constraints requires that the amplitude ratio A_α/A_β should be the same at F_0 and F_{max}. It is very unlikely that upon a short reduction of Q_A structural rearrangements of the Chl protein antenna complexes occur, which would lead to a significant change in the relative amount of Chls coupled to either of the two PS II pools. This constraint is expected to reduce the number of solutions, as the A_α/A_β amplitude ratios for the different solutions are quite different. The second constraint assumes that the lifetime for PS I emission should be the same at F_0 and F_{max}. Making this assumption should reduce a possible interference between the PS I lifetime component and similar PS II kinetics at F_0. By introducing these two constraints a new combined global target analysis was performed. In this approach F_0 and F_{max} data were fitted simultaneously, allowing for different PS II kinetics at F_0 and F_{max}, but restricting the total data set by the two additional constraints discussed above. Starting from each of the six possible combinations of the separate target analyses of F_0 and F_{max}, as listed in Table 1, only one solution was found. The DAS corresponding to this solution are shown in Fig. 5, the values for the rate constants are given in Fig. 6. The reduced χ^2-value for this combined (F_0 and F_{max}) global target analysis is 1.0662.

Assignment and stoichiometry of PS IIα and PS IIβ

For the assignment of α and β to the two different pools of PS II assumed in this target analysis, we again postulate that the majority of the PS II Chls are

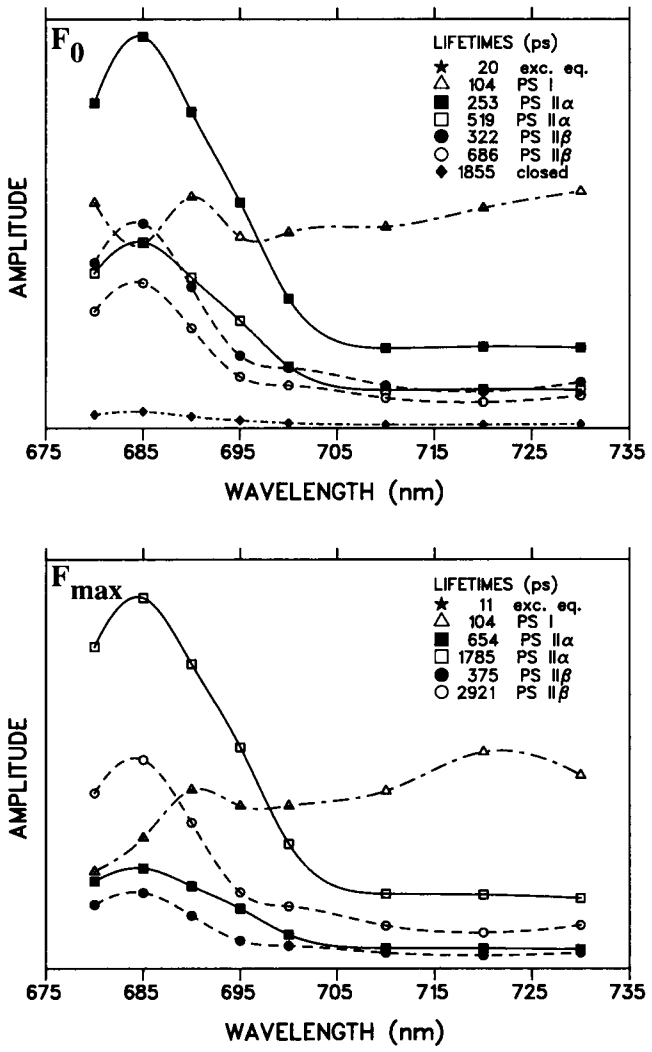

FIGURE 5 DAS of pea chloroplasts at F_0 and F_{max}, as calculated from the corrected amplitudes of the lifetime components resulting from the combined global target analyses. The curves between the data points are interpolated with third-order polynomials. The DAS of the exciton equilibration components (20 ps at F_0 and 11 ps at F_{max}) have a dominant amplitude over the whole spectrum and are not shown here.

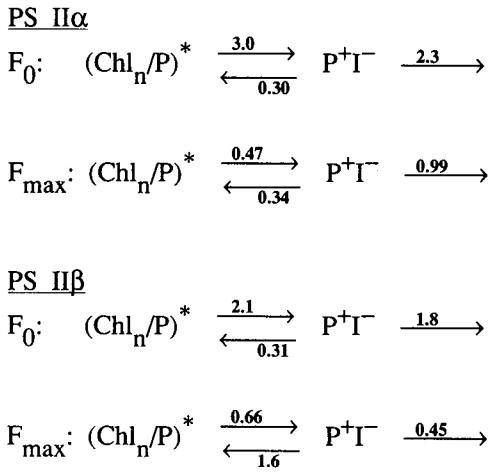

FIGURE 6 Optimal values for the rate constants k_i (ns^{-1}) of PS IIα and PS IIβ at F_0 and F_{max} as resulting from the combined global target analysis of the fluorescence kinetics of pea chloroplasts in terms of a heterogeneous exciton/radical pair equilibrium model. For k_A a value of 0.3 ns^{-1} is assumed.

connected to PS IIα. The amplitude ratio A_α/A_β resulting from the combined global target analysis is 1.9 ± 0.4 (averaged over the whole spectrum, see above). Assuming that at 630 nm Chl *a* and Chl *b* are excited equally strong, these amplitude factors are proportional to the number of Chls in each pool. This means that the α-pool contains twice as many Chls as the β-pool. Assuming antenna sizes of 250 and 100 Chls per reaction center for PS IIα and PS IIβ, respectively (39), it follows that the stoichiometric ratio of PS IIα and PS IIβ reaction centers should be close to unity. Fig. 5 also shows that no significant difference in the emission spectra of PS IIα and PS IIβ could be resolved.

PS IIα is characterized by lifetimes of 0.25 ns (68%) and 0.52 ns (32%) at F_0, which change to 0.65 ns (22%) and 1.79 ns (78%) upon closing the reaction centers (in parentheses the relative amplitudes of the two lifetime components normalized within each PS II type are given). PS IIβ shows lifetimes of 0.32 ns (59%) and 0.67 ns (41%) for open centers, which are lengthened to 0.38 ns (26%) and 2.92 ns (74%) at F_{max}. In previous fluorescence kinetics studies, where only two PS II lifetimes components were resolved both at F_0 and F_{max} (30, 37), the dominant PS II component (0.3 ns at F_0 and 2 ns at F_{max}) was assigned to α-centers, the minor PS II component (0.5 ns at F_0 and 0.6 ns at F_{max}) to β-centers. As it has become clear in the present study that these two lifetime components actually represent a mixture of four, it can be understood why the α/β-assignment at F_{max} in previous work has been somewhat different.

PS I emission

In the combined global target analysis, the PS I emission is fitted with a single lifetime component of 104 ps (Fig. 5). The fit quality at 720 and 730 nm, both at F_0 and F_{max}, as well as the quality of the fit at 680 nm at F_0, is significantly worse than that at the other wavelengths. This could be explained by the fact that in our analysis the PS I emission is assumed as a single exponential component. From fluorescence studies on detergent-

free PS I membrane preparations from spinach (which are thought to be comparable to the in vivo situation for PS I) it is known that (apart from energy transfer processes) the PS I fluorescence decay shows two components with lifetimes of ~60 and ~140 ps (40). The corresponding DAS exhibited quite different amplitude ratios $A_{685\,nm}/A_{720\,nm}$. This might explain why the single-exponential-approximation used here, leads to the wavelength-dependent fit quality mentioned above. However, allowing for two PS I lifetime components in the target analysis procedure would probably not improve the resolution of the PS II kinetics (see also error analysis). It should be noted however, that the shape of the PS I spectrum resolved here is very similar to the composed spectrum (vide supra) of PS I membrane fractions isolated from spinach (40).

Kinetic and energetic parameters of PS II centers

Having found the optimal values for the different rate constants for α- and β-centers, both at F_0 and F_{max} (Fig. 6) we can now discuss in detail the primary kinetics and energetics of these two types of PS II. Before doing so, it proves useful to extract some more detailed information from the set of rate constants. First, it has to be recognized that the rate constant for charge separation, k_1, as used in the exciton/radical pair equilibrium model, includes the partition of the exciton between P^* and all the antenna Chl molecules, Chl_n^*. Therefore k_1 is the apparent rate constant, which is proportional to the intrinsic rate constant for charge separation in the hypothetical isolated reaction center devoid of any antenna pigments. This proportionality is described by an entropy factor (reflecting the N-fold degeneracy of the Chl antenna system) and the Boltzmann-distributed population probabilities for antenna Chls and P, respectively, according to (1):

$$k_1^{int} = k_1 \cdot N \cdot \exp[-hc/kT(\lambda_{Chl}^{-1} - \lambda_P^{-1})], \qquad (1)$$

where h is Planck's constant, c is the light velocity in vacuum, k is the Boltzmann's constant, T, the absolute temperature, and N, the number of Chls in the antenna with maximal absorption at λ_{Chl}, whereas λ_P is the absorption maximum of P (1). In a first approximation, we assumed for both types of PS II a homogeneous Chl antenna composition with maximal absorption at 673 nm, whereas for P we assumed an absorption maximum at 680 nm. Antenna sizes for PS IIα and PS IIβ of 250 and 100 Chls, respectively (39) were assumed. This resulted in proportionality factors k_1^{int}/k_1 of 113 for α-centers and 45 for β-centers. The rather simplifying assumptions made above could be refined, taking into account the heterogeneous antenna composition of PS II, in terms of the PS II core complex (containing 40–60 Chls *a* [41]) and the light harvesting Chl protein complex (called LHCP II, containing Chl *a* and *b* [42]). However, due to the lack of unambiguous information on the spectral properties and possible exciton coupling of these Chl *a* and *b* species in the LHCP II complexes (see e.g. [43,44]) these considerations will not lead to a more refined estimation of the proportionality constants k_1^{int}/k_1 for α- and β-units at present. It has to be noted that the conclusions drawn in this study are not affected qualitatively by the assumptions discussed above. The evaluation of k_1^{int} allows for a comparison between the primary kinetics of PS IIα and PS IIβ, corrected for their different antenna sizes, as well as for a comparison with the experimentally accessible data on the primary kinetics and energetics of the isolated D_1-D_2-Cyt-b_{559} reaction center complex.

We can furthermore evaluate the change in standard free energy accompanying the primary change separation step, ΔG_{cs}^0. If we assume equilibrated states, this can be calculated according to:

$$\Delta G_{cs}^0 = -kT \cdot \ln(k_1/k_{-1}). \qquad (2)$$

Both the free energy change for charge separation in the intact photosystems, $\Delta G_{cs,ps}^0$ can be calculated (using k_1), as well as for charge separation in the hypothetical isolated reaction center $\Delta G_{cs,rc}^0$ (using k_1^{int}). An additional useful parameter, reflecting the efficiency of the separation in open reaction centers is the yield of the charge stabilized state, $\phi(P^+IQ_A^-)$ (the actual yield of the charge stabilized state $\phi(P^+IQ_A^-)$ is probably somewhat lower than the value calculated from the rate constants extracted from fluorscence decay data, as k_2 describes the sum of charge stabilization, radical pair recombination to the ground state and triplet radical pair formation [vide infra]). Related to this parameter is the maximal transient concentration of the radical pair, $(P^+I^-)_{max}$. These parameters can also be determined from the set of fitted rate constants. Finally, we define the average fluorescence lifetime τ_{av} for each type of photosystem according to:

$$\tau_{av} \equiv \sum_{i=1}^{n} A_i \cdot \tau_i \Big/ \sum_{i=1}^{n} A_i, \qquad (3)$$

where A_i and τ_i are the amplitudes and lifetimes of the components originating from this photosystem. As the fluorescence quantum yield of the photosystem is proportional to τ_{av} ($\phi_f = \Sigma_{i=1}^{n} A_i \cdot \tau_i$), we can evaluate the increase in fluorescence quantum yield upon closing the photosystems, i.e., the F_{max}/F_0-ratios for PS IIα and PS IIβ.

Characterization of the primary processes in PS IIα and PS IIβ

In Table 2 the values for the different kinetic and energetic parameters for PS IIα and PS IIβ are collected. In combination with Fig. 6, this allows for a detailed discussion of the primary processes in the two types of PS II.

Although at a first glance it seems that the charge separation rate (i.e., k_1) in both types of PS II (i.e., k_1) are comparable, correcting for the different antenna sizes reveals remarkable differences. For the hypothetical isolated PS IIα reaction center with oxidized Q_A, an intrinsic charge separation time ($1/k_1^{int}$ of 2.9 ps is calculated. This value corresponds well with the lifetime of 3 ps experimentally found in the D_1-D_2-Cyt-b_{559} PS II reaction center complex (2, 3). However, in the isolated PS IIβ reaction center the corresponding process is slower by approximately a factor of 4 (i.e., $1/k_1^{int}$ = 11 ps). The charge recombination process seems to be similar for α- and β-centers, when Q_a is oxidized. Despite the slowed-down charge separation process in β-reaction centers, as compared to α-centers, the quantum efficiency of this process is very similar: in PS IIβ the charge stabilized state $P^+IQ_A^-$ is formed with a yield of 86%, as compared to 90% in PS IIα. Also the maximal transient concentration of the radical pair state P^+I^-, both at F_0 (38% in PS IIα, 35% in PS IIβ) and F_{max} (17% in PS IIα and 18% in PS IIβ) are very similar for the two types of PS II.

TABLE 2 Kinetic and energetic parameters for PS IIα and PS IIβ at F_0 and F_{max}, as revealed by the combined global target analysis of the fluorescence kinetics of chloroplasts at F_0 and F_{max}

	PS IIα		PS IIβ	
	F_0	F_{max}	F_0	F_{max}
$1/k_1^{int}$ (ps)	2.9	19	11	34
$\phi(P^+IQ_A^-)$	90%		86%	
$(P^+I^-)_{max}$	38%	17%	35%	18%
$\Delta G^0_{cs,ps}$ (meV)	−55	−8	−46	21
$\Delta G^0_{cs,rc}$ (meV)	−168	−121	−138	−71
τ_i (ns), A_i	0.25 (68%)	0.65 (22%)	0.32 (59%)	0.38 (26%)
	0.52 (32%)	1.79 (78%)	0.67 (41%)	2.92 (74%)
F_{max}/F_0	4.6		4.9	

$1/k_1^{int}$ is the (extrapolated) charge separation time in the isolated reaction centers; $\phi(P^+IQ_A^-)$ is the quantum yield of charge stabilization in open reaction centers; $(P^+I^-)_{max}$ is the maximal transient concentration of the primary radical pair state; $\Delta G^0_{cs,ps}$ is the free energy change for charge separation in intact photosystems; $\Delta G^0_{cs,rc}$ is the free energy change for charge separation in the isolated reaction center; the relative amplitudes A_i (in parentheses) of the lifetime components τ_i are normalized to 100% for each type of PS II; F_{max}/F_0 is the ratio of the fluorescence quantum yield of closed to open reaction centers.

Upon reduction of Q_A, the charge separation process in α-centers is slowed down by a factor of 6, whereas the rate constant for charge recombination, k_{-1}, is increased only slightly (Fig. 6). For β-centers a distinctly different behavior is found. Closing the β-reaction center makes k_1 drop by factor of 3, whereas the charge recombination process become faster by a factor of 5 (k_{-1} = 1.6 ns^{-1}). The negative charge on Q_A^- in closed centers results in an increase of the radical pair standard free energy, relative to the excited state $(Chl_n/P)^*$ (which is assumed not to change in free energy), of 47 meV (from −55 to −8 meV) and 67 meV (from −46 to 21 meV) in α-centers and β-centers, respectively. For the hypothetical isolated PS II reaction centers the charge separation in open centers (Q_A oxidized) is accompanied by a change in standard free energy of −168 meV in PS IIα and −138 meV in PS IIβ (Table 2). In the experimentally isolated D_1-D_2-Cyt-b_{559} reaction center complex of PS II (devoid of any quinone) ΔG^0_{cs} was measured to be −110 meV (45) and −124 meV (3). These values are smaller than the extrapolated values reported here. The reason for this is unclear at present.

The changes of the rate constants upon closing the α-centers are very similar to those observed previously in (homogeneous) PS II particles from the cyanobacterium *Synechococcus sp.* (1). In these particles the reduction of Q_A was found to lead to a six-fold decrease in k_1 and only a 20% increase in k_{-1}, which corresponds to a lift in free energy of 50 meV. On the other hand, a behavior, similar to that found here for PS IIβ, has been reported for destacked thylakoid membranes (BBY's) from peas. Leibl et al. (17) measured the picosecond photovoltage kinetics from PS II membranes which were destacked by a mild trypsin digestion. Combined with the fluorescence decay kinetics of these samples, they used these data to calculate the molecular rate constants for the homogeneous excited state/radical pair equilibrium model. It was found that closing the PS II reaction center leads to a three-fold decrease of the charge separation rate, whereas the charge recombination process was accelerated by a factor of 8. The corresponding free energy increase of the radical pair was 77 meV. It has to be noted here that in the analysis by Leibl et al. a homogeneous PS II pool was assumed (17).

The effect of Q_A reduction on the kinetics of the primary charge separation and charge recombination is thought to be the result of Coulombic interactions between the negative charge on Q_A^- and the radical pair P^+I^- (1, 17). The different behavior of PS IIα and PS IIβ upon reduction of Q_A indicates a different structural arrangement of the reaction center pigments for both types of PS II and/or a different local environment in

and around the reaction center (see Conclusions and Perspectives).

Regulation of the deactivation rate of the radical pair P^+I^- at F_0 and F_{max}

As already pointed out in the Introduction, fitting the exciton/radical pair equilibrium model to fluorescence decay kinetics at F_0, leads to k_2 actually describing the sum of three processes: charge stabilization (electron transfer from I^- to Q_A) on the one hand and radical pair recombination to the ground state and triplet radical pair formation on the other hand. At F_{max}, k_2' solely describes the deactivation of the singlet radical pair to triplet and/or ground states. Having found a solution for the rate constants (Fig. 6) we can compare the values for k_2 and k_2', in other words the situation at F_0 and F_{max}. As at F_0 the charge stabilized state $P^+IQ_A^-$ is formed with a very high yield, the rate constants for the radical pair deactivation pathways to triplet and/or ground states, must be smaller than the rate constant for charge stabilization by at least one order of magnitude. This sets an upper limit for the deactivation rate constants in PS IIα and PS IIβ of $\sim 0.2\ ns^{-1}$. Comparing this value with the values found for k_2' (the sum of the singlet radical pair deactivation rate constants at F_{max}), i.e., 0.99 ns^{-1} for PS IIα and 0.45 ns^{-1} for PS IIβ, shows that these processes have become faster upon reduction of Q_A by a factor of ~ 2 (PS IIβ) and ~ 5 (PS IIα), respectively. Whether the triplet radical pair formation or the recombination of the singlet radical pair to the ground state, or both, get accelerated cannot be determined from this analysis. It seems, however, that the increase of the singlet radical pair deactivation rate constants upon reduction of Q_A^- provides an additional regulation mechanism for PS II to deactivate radical pair states in closed centers. This aspect deserves further investigations in the future.

Stationary fluorescence quantum yield: variable fluorescence

The increase in fluorescence quantum yield upon closing the centers, as can be calculated from the rate constants, is comparable for both types of PS II. For PS IIα a F_{max}/F_0-ratio of 4.6 was calculated, whereas for PS IIβ a value of 4.9 resulted. This fact that PS IIα and PS IIβ have almost identical F_{max}/F_0-ratios is commonly assumed in the analysis of fluorescence induction curves in the presence of DCMU (27, 28), without any experimental evidence so far. Our results provide the first experimental support for this assumption. We further want to emphasize here that the discussion of the mechanistic origins of variable fluorescence in PS II (i.e., the increase from F_0 to F_{max}) should be reformulated, taking into account the insights gained by the model descriptions on a molecular level. Posing delayed fluorescence (caused by an increased charge recombination; Klimov et al. [46, 47]) versus prompt fluorescence (Schatz et al. [1, 15]; Moya et al. [48]) has become mere semantics. From the results presented here, it is obvious that two different types of PS II must be taken into account. We also want to stress here that the commonly used assumption that the variable fluorescence, F_v, is a superposition of a constant F_0-level and an increased fluorescence yield caused by closing the PS II reaction centers ($F_v \equiv F - F_0$), is physically meaningless. There is no F_0-level present in any state that has a fluorescence quantum yield above F_0. The fluorescence yield at F_0 results from a particular set of molecular rate constants for the primary processes and this quantum yield changes as soon as one or more of the rate constants are changed upon closure of the PS II reaction centers (reduction of Q_A).

Error ranges of the set of rate constants

As described in Materials and Methods, we performed two kinds of error analyses on the results from the combined global target analysis (Fig. 6). In these procedures we calculated the ranges in which each rate constant could be varied without significantly decreasing the fit quality. We applied a confidence level of 67% (roughly corresponding to one standard deviation). This results in an F-factor of 1.0077 (for $\sim 13{,}000$ degrees of freedom in this combined global target analysis).

If we do not account for any correlation between the fit parameters (unidimensional search procedure), none of the rate constants describing the kinetics of open centers (F_0) could be varied (increased or decreased) by more than 3% without causing a significant loss of fit quality. For the rate constants at F_{max} this limit was 2%. In all cases (F_0 and F_{max}, α- and β-centers) the charge separation rate constant k_1 shows error ranges of $< 1\%$. These results suggest that the accuracy of the values found for the rate constants is very good, but is nevertheless not the same for all types of rate constants (vide infra).

The error ranges resulting from the exhaustive search error analysis (accounting for all possible correlations between the fit parameters) are listed in Table 3. It is obvious that this procedure recovered enormously large error ranges for all the rate constants, as compared to the unidimensional search procedure. But also from the exhaustive search procedure it resulted that the rate constant for charge separation, k_1, is the most restricted

TABLE 3 **Rate constants (bold; ns^{-1}) and error ranges for PS IIα and PS IIβ at F_0 and F_{max}, as resulted from the exhaustive search error analysis procedure with a 67% confidence level (see Materials and Methods) in the combined global target analysis**

	PS IIα		PS IIβ	
F_0:				
k_1	**3.0**	2.2 – 3.9	**2.1**	1.6 – 4.8
k_{-1}	**0.30**	0.030 – 0.75	**0.31**	<0.03 – 1.4
k_2	**2.3**	1.1 – 3.5	**1.8**	1.1 – >18
F_{max}:				
k_1	**0.47**	0.33 – 2.4	**0.66**	<0.07 – 2.9
k_{-1}	**0.34**	<0.03 – >3.4	**1.6**	<0.2 – >16
k_2'	**0.99**	0.49 – >10	**0.45**	0.33 – >4.5

If a rate constant could be deviated from its optimal value by more than one order of magnitude, this is given as upper/lower limit.

one (i.e., has the smallest error range). The rate constant for charge recombination, however, shows large error ranges, in most cases even more than one order of magnitude. In general, the rate constants for the α-centers are better defined than the corresponding ones for the β-centers. This can be explained, inter alia, by the smaller pool size for the latter.

During the exhaustive search, no reduced χ^2-value smaller than χ^2_{min} (corresponding to the optimal solution) was found. This indicates that (within the range covered by this procedure) there exists only one minimum on the χ^2-surface, or in other words, the solution found here is indeed unique. The fact that the exhaustive search analysis recovered much larger error ranges than the unidimensional search procedure, shows that there exist significant correlations between the different fit parameters. These correlations can act among the rate constants for one type of PS II, between the rate constants for the different types of PS II, or between the PS II kinetics and the PS I kinetics. To allocate these correlations more precisely, additional semi-exhaustive searches would have to be performed.

From the results of the different error analysis procedures, as presented here, it has become evident that merely calculating standard errors (from the curvature matrix at χ^2_{min}) or searching unidimensionally, i.e., not taking into account the correlations between the fit parameters, results in error ranges that are completely useless. Only if all possible correlations are accounted for, a more realistic description of the accuracy of the solution for the fit parameters emerges.

Heterogeneous bipartite model

As discussed in the Introduction, both the bipartite model (12) and the exciton/radical pair equilibrium model (1) predict biexponential fluorescence kinetics for a homogeneous pool of PS II. This enables us to try for an alternative interpretation of the rate constants recovered in the combined target analysis by application of the heterogeneous bipartite model. In the bipartite model k_1 and k_{-1} would represent forward and backward energy transfer rates from the Chl antenna system to the reaction center complex. However, the values found here for open reaction centers imply that these energy transfer processes would take place on a time scale of several hundreds of picoseconds. This would be very inefficient for such a specialized light harvesting system. Moreover, the decrease of the rate constant for forward energy transfer, as observed upon closing the centers (transfer times of ~2 ns), would imply a drastic rearrangement of the antenna complexes relative to the reaction center complex. This would be even harder to rationalise. At F_{max} only a small fraction of the excitation energy would reach the reaction center, as k_1 would have to compete with k_A being 0.3 ns^{-1}. On the other hand, in the bipartite model, the rate constant k_2 (and k_2') would reflect the charge separation process in the isolated reaction center. The values found here for open centers, however, would correspond to a charge separation time of ~500 ps, which is two orders of magnitudes too slow if compared to recent experimental values (2, 3) and is also unreasonably slow in light of the high quantum yield for producing the charge separated state. These considerations clearly show that the application of the (heterogeneous) bipartite model to the fluorescence kinetics of chloroplasts results in a physically highly unreasonable situation. Therefore this model is inadequate in describing the primary photophysics and photochemistry in PS II of higher plant thylakoids.

CONCLUSIONS AND PERSPECTIVES

We have analyzed the fluorescence decay kinetics of chloroplasts at F_0 and F_{max} in terms of a heterogeneous exciton/radical pair equilibrium model. The differences found between PS IIα and PS IIβ can clearly not be explained solely by a difference in antenna size (39), as has been assumed thus far. They imply a different molecular functioning of the two photosystems. This could either mean that the reaction center structure is different and thus its photochemical performance. Alternatively, it could mean that the same reaction center structure would be located in two different environments and thus function differently. It has been suggested that PS IIα is exclusively located in the grana regions of the thylakoid membrane, whereas PS IIβ should be located in the stroma regions (49). If so, it can be easily rationalized that these two environments have

different effects on the kinetics and energetics of the primary photochemistry of the PS II centers located in each environment. As discussed above, the characteristics attributed to PS IIβ were also found in destacked BBY membranes (17). This makes it tempting to suggest that PS IIβ are those PS II systems that are located in the nonappressed region, i.e., destacked grana membranes, as well as the stroma region of in vivo thylakoid membranes. They not only have a smaller antenna size (less LHCP II), but also a different local environment in terms of, e.g., membrane potential, surface charge density, ionic strength. This working hypothesis would imply that PS IIα are those PS II complexes located in the appressed regions of the thylakoid membrane. However, at present it is hard to understand why isolation of a PS II particle by detergent treatment (1, 5), would create a local environment similar to that in appressed thylakoid membranes. We therefore have to conclude that, although this study presents remarkable differences between the primary kinetics of PS IIα and PS IIβ, the molecular basis for these differences is still poorly understood. Whether differences in reaction center structure or in local environment, or both, form the origin needs to be elucidated by further experiments. An interesting and promising approach would be to alter the thylakoid membrane structure in a controlled manner (e.g., stacking/destacking, phosphorylation) to uncover a presumed relationship between the thylakoid structure and the two types of kinetic and energetic behavior found for PS IIα and PS IIβ. Such experiments have been performed in the past, e.g., (14, 50–53), but the quality of these data probably does not allow for the extensive data analysis needed here.

Further experiments are also needed to improve the accuracy of the recovered values for the different rate constants (Table 3). The fluorescence decay curves used in this study have a very high signal to noise (S/N) ratio (65,000 count in the peak channel). As the S/N-ratio increases with the square root of the number of counts and thus with the square root of the measuring time, further extension of the measuring time per curve (up to 75 min per curve needed here) comes to a limit, set by the stability of the single photon timing system, as well as that of the sample and/or by the variance between different batches of chloroplast preparations. Also, in this study we used the spectral information to its maximum extent. No significant differences could be detected in the emission spectra of the two types of PS II. So, neither collecting more data per decay curve, nor recording at more emission wavelengths, is expected to result in a significant improvement of the information content of the data set acquired. An approach that seems to be more promising is combining different excitation wavelengths, as the antenna system of PS IIα is thought to contain more Chl *b* in its antenna system, as compared to PS IIβ (49). Exciting at different wavelengths thus varies the relative absorption cross sections of PS IIα and PS IIβ. Also the above mentioned controlled manipulation of the thylakoid membrane could decrease the error ranges for the different rate constants, as far as correlations between the fit parameters of α- and β-centers is significant.

The approach to PS IIα and PS IIβ, as presented in this study can also be applied to more physiological phenomena such as energy quenching, photoinhibition, state transitions, et cetera, as there are indications that the two types of PS II are affected to a different extent. We emphasize here that all possible differences between the functioning of PS IIα and PS IIβ that might go beyond the reduction of Q_A (such as *B*-type/non *B*-type, active/inactive, et cetera; see 54 for a review) cannot be monitored with the methods used in this study. As far as primary charge separation and charge stabilization (to $P^+IQ_A^-$) are concerned, both PS II units are highly efficient.

We want to acknowledge Iris Martin, who programmed the target analysis procedure and gave continuous support during the several extensions that were needed. Furthermore we thank Ethel Hüttel and Uli Pieper for assistance during the SPT experiments. T. A. Roelofs acknowledges Professor H.-W. Trissl for stimulating discussions. Professor K. Schaffner is acknowledged for his support of this work.

Received for publication 16 August 1991 and in final form 30 December 1991.

REFERENCES

1. Schatz, G. H., H. Brock, and A. R. Holzwarth. 1988. A kinetic and energetic model for the primary processes in photosystem II. *Biophys. J.* 54:397–405.
2. Wasielewski, M. R., D. G. Johnson, M. Seibert, and Govindjee. 1989. Determination of the primary charge separation rate in isolated photosystem II reaction centers with 500-fs time resolutions. *Proc. Natl. Acad. Sci. USA.* 86:524–528.
3. Roelofs, T. A., M. Gilbert, V. A. Shuvalov, and A. R. Holzwarth. 1991. Picosecond fluorescence kinetics of the D1-D2-Cyt-b559 photosystem II reaction center complex: energy transfer and primary charge separation processes. *Biochim. Biophys. Acta.* 1060:237–244.
4. Nuijs, A. M., H. J. van Gorkom, J. J. Plijter, and L. N. M. Duysens. 1986. Primary-charge separation and excitation of chlorophyll a in photosystem II particles from spinach as studied by picosecond absorbance-difference spectroscopy. *Biochim. Biophys. Acta.* 848:167–175.
5. Schatz, G. H., H. Brock, and A. R. Holzwarth. 1987. Picosecond kinetics of fluorescence and absorbance changes in photosystem II particles excited at low photon density. *Proc. Natl. Acad. Sci. USA.* 84:8414–8418.

6. Trissl, H.-W., and W. Leibl. 1989. Primary charge separation in photosystem II involves two electrogenic steps. *FEBS (Fed. Eur. Biochem. Soc.) Lett.* 244:85–88.

7. Debus, R. J., B. A. Barry, I. Sithole, G. T. Babcock, and L. McIntosh. 1988. Directed mutagenesis indicates that the donor to P+680 in photosystem II is tyrosine-161 of the D1 polypeptide. *Biochemistry.* 27:9071–9074.

8. Metz, J. G., P. J. Nixon, M. Rögner, G. W. Brudvig, and B. A. Diner. 1989. Directed alteration of the D1 polypeptide of photosystem II: evidence that tyrosine 161 is the redox component, *Z*, connecting the oxygen-evolving complex to the primary electron donor, P 680. *Biochemistry.* 28:6960–6969.

9. Hoff, A. J. 1986. Magnetic interactions between photosynthetic reactants. *Photochem. Photobiol.* 43:727–745.

10. Van Gorkom, H. J. 1985. Electron transfer in photosystem II. *Photosynt. Res.* 6:97–112.

11. Hansson, Ö., and T. Wydrzynski. 1990. Current perceptions of photosystem II. *Photosynth. Res.* 23:131–162.

12. Butler, W. L., D. Magde, and S. J. Berens. 1983. Fluorescence lifetimes in the bipartite model of the photosynthetic apparatus with alpha, beta heterogeneity in photosystem II. *Proc. Natl. Acad. Sci. USA.* 80:7510–7514.

13. Berens, S. J., J. Scheele, W. L. Butler, and D. Magde. 1985. Kinetic modeling of time resolved fluorescence in spinach chloroplasts. *Photochem. Photobiol.* 42:59–68.

14. Berens, S. J., J. Scheele, W. L. Butler, and D. Magde. 1985. Time-resolved fluorescence studies of spinach chloroplasts. Evidence for the heterogeneous bipartite model. *Photochem. Photobiol.* 42:51–57.

15. Schatz, G. H., and A. R. Holzwarth. 1986. Mechanisms of chlorophyll fluorescence revisited: prompt or delayed emission from photosystem II with closed reaction centers? *Photosynth. Res.* 10:309–318.

16. Trissl, H.-W., J. Breton, J. Deprez, and W. Leibl. 1987. Primary electrogenic reactions of photosystem II as probed by the light-gradient method. *Biochim. Biophys. Acta.* 893:305–319.

17. Leibl, W., J. Breton, J. Deprez, and H.-W. Trissl. 1989. Photoelectric study on the kinetics of trapping and charge stabilization in oriented PS II membranes. *Photosynth. Res.* 22:257–275.

18. Holzwarth, A. R. 1991. Excited state kinetics in chlorophyll systems and its relationship to the functional organization of the photosystems. *In* Chlorophylls. CRC Handbook. H. Scheer, editor. CRC Press, Boca Raton, FL. 1125–1151.

19. McCauley, S. W., E. Bittersmann, and A. R. Holzwarth. 1989. Time-resolved ultrafast blue-shifted fluorescence from pea chloroplasts. *FEBS (Fed. Eur. Biochem. Soc.) Lett.* 249:285–288.

20. Van Grondelle, R. 1985. Excitation energy transfer, trapping and annihilation in photosynthetic systems. *Biochim. Biophys. Acta.* 811:147–195.

21. Geacintov, N. E., and J. Breton. 1987. Energy transfer and fluorescence mechanisms in photosynthetic membranes. *CRC Crit. Rev. Plant Sci.* 5:1–44.

22. Roelofs, T. A., and A. R. Holzwarth. 1990. In search of a putative long-lived relaxed radical pair state in closed photosystem II. Kinetic modeling of picosecond fluorescence data. *Biophys. J.* 57:1141–1153.

23. McCauley, S. W., E. Bittersmann, M. G. Müller, and A. R. Holzwarth. 1990. Picosecond chlorophyll fluorescence from higher plants. *In* Current Research in Photosynthesis, Vol. II. M. Baltscheffsky, editor. Kluwer Academic Publishers, Dordrecht. 297–300.

24. Hodges, M., and I. Moya. 1986. Time-resolved chlorophyll fluorescence studies of photosynthetic membranes: resolution and characterization of four kinetic components. *Biochim. Biophys. Acta.* 849:193–202.

25. Beechem, J. M., M. Ameloot, and L. Brand. 1985. Global and target analysis of complex decay phenomena. *Anal. Instrum.* 14:379–402.

26. Beechem, J. M., E. Gratton, M. Ameloot, J. R. Knutson, and L. Brand. 1992. The global analysis of fluorescence intensity and anisotropy decay data: second generation theory and programs. *In* Topics in Fluorescence Spectroscopy. Vol. 2: Principles. J. R. Lakowicz, editor. Plenum Publishing Corp., New York. In press.

27. Melis, A., and P. H. Homann. 1976. Heterogeneity of the photochemical centers in system II of chloroplast. *Photochem. Photobiol.* 23:343–350.

28. Melis, A., and P. H. Homann. 1975. Kinetic analysis of the fluorescence induction in 3-(3,4-dichlorophenyl)-1,1-dimethylurea poisoned chloroplasts. *Photochem. Photobiol.* 21:431–437.

29. Glick, R. E., S. W. McCauley, and A. Melis. 1985. Effect of light quality on chloroplast-membrane organization and function in pea. *Planta.* 164:487–494.

30. Wendler, J., and A. R. Holzwarth. 1987. State transitions in the green alga Scenedesmus obliquus probed by time-resolved chlorophyll fluorescence spectroscopy and global data analysis. *Biophys. J.* 52:717–728.

31. Holzwarth, A. R., J. Wendler, and W. Haehnel. 1985. Time-resolved picosecond fluorescence spectra of the antenna chlorophylls in Chlorella vulgaris. Resolution of photosystem I fluorescence. *Biochim. Biophys. Acta.* 807:155–167.

32. Eads, D. D., S. P. Webb, T. G. Owens, L. Mets, R. S. Alberte, and G. R. Fleming. 1987. Characterization of the fluorescence decays of the chlorophyll *a*/*b* protein. *In* Progress in Photosynthesis Research, Vol. I. J. Biggins, editor. Nijhoff, Dordrecht. 135–138.

33. Ide, J. P., D. R. Klug, W. Kühlbrandt, L. B. Giorgi, and G. Porter. 1987. The state of detergent solubilised light-harvesting chlorophyll-*a*/*b* protein complex as monitored by picosecond time-resolved fluorescence and circular dichroism. *Biochim. Biophys. Acta.* 893:349–364.

34. Marquardt, D. W. 1963. An algorithm for least-squares estimation of nonlinear parameters. *J. Soc. Ind. Appl. Math.* 11:431–441.

35. Johnson, M. L. 1983. Evaluation and propagation of confidence intervals in nonlinear, asymmetrical variance spaces. Analysis of ligand-binding data. *Biophys. J.* 44:101–106.

36. Pugh, E. M., and G. H. Winslow. 1966. The analysis of physical measurements. Addison-Wesley Publishing Company, Inc., Reading, Mass.

37. Schatz, G. H., and A. R. Holzwarth. 1987. Picosecond time resolved chlorophyll fluorescence spectra from pea chloroplast thylakoids. *In* Progress in Photosynthesis Research, Vol. I. J. Biggins, editor. Nijhoff, Dordrecht. 67–69.

38. Lee, C.-H., T. A. Roelofs, and A. R. Holzwarth. 1990. Target analysis of picosecond fluorescence kinetics in green algae: characterization of primary processes in photosystem II alpha and beta. *In* Current Research in Photosynthesis, Vol. I. M. Baltscheffsky, editor. Kluwer Academic Publishers, Dordrecht. 387–390.

39. Melis, A., and J. M. Anderson. 1983. Structural and functional organization of the photosystems in spinach chloroplasts. Antenna size, relative elctron-transport capacity, and chlorophyll composition. *Biochim. Biophys. Acta.* 724:473–484.

40. Holzwarth, A. R., W. Haehnel, R. Ratajczak, E. Bittersmann, and G. H. Schatz. 1990. Energy transfer kinetics in photosystem I particles isolated from *Synechococcus sp.* and from higher plants. *In* Current Research in Photosynthesis, Vol. II. M. Baltscheffsky, editor. Kluwer Academic Publishers, Dordrecht. 611–614.

41. Satoh, K. 1985. Protein-pigments and photosystem II reaction center. *Photochem. Photobiol.* 42:845–853.

42. Butler, P. J. G., and W. Kühlbrandt. 1988. Determinations of the aggregate size in detergent solution of the light-harvesting chlorophyll *a*/*b*-protein complex from chloroplast membranes. *Proc. Natl. Acad. Sci. USA.* 85:3797–3801.

43. Kühlbrandt, W., and D. N. Wang. 1991. Three-dimensional structure of plant light-harvesting complex determined by electron crystallography. *Nature (Lond.).* 350:130–134.

44. Hemelrijk, P. W., S. L. S. Kwa, R. van Grondelle, and J. P. Dekker. 1991. Spectroscopic properties of LHC-II, the main light-harvesting chlorophyll *a*/*b* protein complex from chloroplast membranes. *Biochim. Biophys. Acta.* 1098:159–166.

45. Booth, P. J., B. Crystall, L. B. Giorgi, J. Barber, D. R. Klug, and G. Porter. 1990. Thermodynamic properties of D1/D2/cytochrome *b*-559 reaction centres investigated by time-resolved fluorescence measurements. *Biochim. Biophys. Acta.* 1016:141–152.

46. Klimov, V. V., A. V. Klevanik, V. A. Shuvalov, and A. A. Krasnovsky. 1977. Reduction of pheophytin in the primary light reaction of photosystem II. *FEBS (Fed. Eur. Biochem. Soc.) Lett.* 82:183–186.

47. Klimov, V. V., and A. A. Krasnovskii. 1982. Participation of pheophytin in the primary processes of electron transfer at the reaction centers of photosystem II. *Biophysics.* 27:186–198.

48. Moya, I., M. Hodges, J.-M. Briantais, and G. Hervo. 1986. Evidence that the variable chlorophyll fluorescence in *Chlamydomonas reinhardtii* is not recombinant luminescence. *Photosyn. Res.* 10:319–325.

49. Anderson, J. M., and A. Melis. 1983. Localization of different photosystems in separate regions of chloroplast membranes. *Proc. Natl. Acad. Sci. USA.* 80:745–749.

50. Nairn, J. A., W. Haehnel, P. Reisberg, and K. Sauer. 1982. Picosecond fluorescence kinetics in spinach chloroplasts at room temperature. Effects of Mg^{2+}. *Biochim. Biophys. Acta.* 682:420–429.

51. Karukstis, K. K., and K. Sauer. 1983. Picosecond fluorescence studies of electron acceptor *Q* redox heterogeneity. *Biochim. Biophys. Acta.* 725:246–253.

52. Haworth, P., K. K. Karukstis, and K. Sauer. 1983. Picosecond fluorescence kinetics in spinach chloroplasts at room temperature. Effects of phosphorylation. *Biochim. Biophys. Acta.* 725:261–271.

53. Briantais, J.-M., M. Hodges, and I. Moya. 1987. Comparison between the effect of cations, state I-state II transitions and protein-phosphorylation on lifetime components of chlorophyll fluorescence. *In* Progress in Photosynthesis Research, Vol. II. J. Biggins, editor. Nijhoff Publishers, Dordrecht. 705–708.

54. Govindjee. 1990. Photosystem II heterogeneity: the acceptor side. *Photosynth. Res.* 25:151–160.